Nanocatalytic chemohydrodynamic instability: Deposition effects

B. Dastvareh*
Department of Mechanical Engineering, University of Alberta, Edmonton, Alberta, Canada T6G 1H9

J. Azaiez†
Department of Chemical and Petroleum Engineering, Schulich School of Engineering, University of Calgary, Calgary, Alberta, Canada T2N 4V8

P. A. Tsai‡
Department of Mechanical Engineering, University of Alberta, Edmonton, Alberta, Canada T6G 1H9

(Received 26 August 2019; published 8 November 2019)

Due to the high surface area to volume ratio of nanoparticles, nanocatalytic reactive flows are widely utilized in various applications, such as water purification, fuel cell, energy storage, and biodiesel production. The implementation of nanocatalysts in porous media flow, such as oil recovery and contaminant transport in soil, can trigger or modify the interfacial instabilities called viscous fingering. These instabilities grow at the interface of the fluids when a less viscous fluid displaces a high viscous one in porous media. Here the flow dynamics and the total amount of chemical product are investigated when two reactive miscible fluids meet in a porous medium while undergoing $A + B + n \rightarrow C + n$ reaction. Nanocatalysts (n) are dispersed in the displacing fluid and deposited gradually with time. Four generic regimes are observed over time as a result of the particle deposition: (1) the initial diffusive regime, where the flow is stable with decreasing production rate, (2) the mixing-dominant fingering regime, where the flow is unstable and the production rate generally increases, (3) the transition regime, where the production rate generally decreases regardless of whether the system is stable or unstable, and (4) the final zero-production regime, where the product diffuses and fades away in the channel. Although the general trend shows a decreasing reaction rate with nanocatalysts deposition, there is a period in which the production rate increases due to the moderate deposition rates. Such an increase of production, however, is not observed in two groups: first, those systems in which the nanocatalysts do not change the viscosity of the base fluid and, second, a subgroup of the systems that are stable before and after the reaction in the absence of deposition.

DOI: 10.1103/PhysRevE.100.053102

I. INTRODUCTION

Nanocatalysts are ultrafine particles that play a catalytic role in reactions. Due to their tremendous surface area to volume ratio, nanocatalysts have the advantage of providing the most optimized sites to accelerate reactions. They are more active than heterogeneous catalysts, while they can be separated from the reaction mixture easier than homogeneous ones. Therefore, the interest in nanocatalytic reactive systems is growing in different applications. For instance, nanocatalysts are widely used in water purification [1], fuel cell [2], renewable energy [3], and biodiesel production [4], to name a few. The growing interest in implementing nanocatalysts in applications such as oil recovery [5,6] and contaminant transport in soil [7] raises the question of whether nanocatalysts influence viscous fingering instabilities. Viscous fingering (VF) is a hydrodynamic instability occurring at the interface of two approaching fluids in porous media when a less viscous fluid displaces a more viscous one.

There are two types of viscous fingering, depending on whether the acting fluids are miscible or immiscible. Concerning miscible viscous fingering, which is the focus of this study, only a few studies have been conducted for nanocatalytic reactive systems. In these studies, nanocatalysts are dispersed in an invading fluid that reacts with a displaced fluid in a porous medium or a Hele-Shaw cell. Systems undergoing $A + n \rightarrow B + n$ reaction have been studied with linear stability analysis and nonlinear simulations [8,9]. It was concluded that the increase in the viscosity of the invading fluid after the addition of nanocatalysts reduces the instability, while higher reaction rates promote the interfacial instability and widen the fingers. In addition, the nanocatalysts efficiency was discussed in terms of the degree of mixing, *in situ* conversion rate of the reactants, and their penetration depth in porous media. Recently the system undergoing the more generic $A + B + n \rightarrow C + n$ reaction has been investigated in the absence of deposition [10]. There the production of the

*Corresponding author: dastvare@ualberta.ca
†azaiez@ucalgary.ca
‡peichun.amy.tsai@ualberta.ca

chemical C changes the dynamics significantly. Based on the viscosity ratio of different components, the authors identified the stability criteria and determined how the fingers of the chemical product C develop after the reaction. Extending the study to account for the heat of reaction, they found that thermophoresis, a transport mechanism of the particles as a result of temperature gradient, has a dramatic effect on both the dynamics and the total chemical product.

The VF in nanocatalytic reactive systems can be categorized as a branch of the general category of chemohydrodynamic instabilities, already studied widely. It was reported that in particle-free autocatalytic reactive systems (A → B), an increase in the viscosity ratio (of the displaced to displacing fluids) and the reaction rate has a destabilizing effect [11,12]. In addition, the enhancement of tip splitting and drop formation were observed in these autocatalytic reactive systems. The generic bimolecular reactive systems undergoing A + B → C have been studied both experimentally [13,14] and theoretically [15], in the rectilinear or radial geometry [16], and with a moderate [17] or very fast reaction rates [18]. Similar to the autocatalytic reactive systems, the reaction rate increases the instability of these systems. Furthermore, the initial concentration and diffusivity of each components influence both the dynamics and VF instability. As an interesting finding, it was reported that if the system is unstable before the reaction, it will remain unstable after the reaction. However, the initially stable system can become unstable or remain stable after the reaction, depending on the values of the viscosity ratio of the chemical product C.

Since nanocatalysts may deposit while moving along the channel, the present study aims to understand how the deposition affects both the dynamics and the total amount of chemical product in a reactive flow undergoing a generic nanocatalytic chemical reaction of A + B + n → C + n. To the best of our knowledge, this phase has not been investigated. To elucidate the underlying mechanism, first, the reactive systems in a porous medium are analyzed based on their categorization whether they are stable or unstable before and after the reaction in the absence of deposition. Subsequently, the response of those systems is analyzed under deposition, in terms of the dynamics and the chemical product.

II. PHYSICAL PROBLEM

The schematic view of the nanocatalytic reactive system undergoing A + B + n → C + n reaction is shown in Fig. 1, representing a homogeneous porous medium or a Hele-Shaw cell. Solution A with initial concentration C_0 is injected into the channel with velocity U, while the solution B with the same initial concentration is at rest. As the two fluids meet, they react in the presence of nanocatalysts (n) dispersed with the initial concentration of C_{n_0} in the displacing fluid. The viscosity of each component at their initial concentrations is μ_{a_0}, μ_{b_0}, and μ_{n_0}, respectively. The resulting component C is a product of A + B + n → C + n chemical reaction, with the viscosity of μ_{c_0} at the concentration C_0. Henceforth, "NP" notation refers to the nanocatalysts.

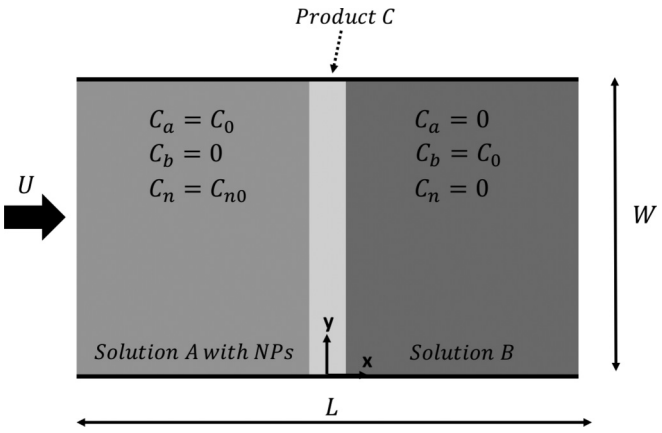

FIG. 1. Schematic diagram of the numerical simulation of nanocatalytic reactive flow undergoing A + B + n → C + n reaction in a porous medium.

III. PROBLEM FORMULATION

The nanocatalytic reactive flow can be accurately formulated by the conservation of mass, Darcy's law, and four advection-diffusion equations governing the transport of each component (A, B, C, and NP). The corresponding dimensionless governing equations in a reference frame moving with the velocity U are [10]

$$\vec{\nabla} \cdot \vec{V} = 0, \tag{1}$$

$$\vec{\nabla} P = -\mu(\vec{V} + \vec{i}), \tag{2}$$

$$\frac{\partial C_j}{\partial t} + \vec{V} \cdot \vec{\nabla} C_j = \delta_j \nabla^2 C_j \pm \mathrm{Da} C_a C_b C_n, \tag{3}$$

$$\frac{\partial C_n}{\partial t} + \vec{V} \cdot \vec{\nabla} C_n = \delta_n \nabla^2 C_n - \mathrm{Da}_{dep} C_n. \tag{4}$$

For Eq. (3), $C_j = (C_a, C_b, C_c)$ is the concentration of each components, i.e., there are three equations in total, modeling the concentrations of A, B, and C. The positive sign for the reaction rate $r_R = \mathrm{Da} C_a C_b C_n$ in Eq. (3) is implemented for the component C, while the negative sign for the components A and B. To derive these dimensionless equations, permeability was first incorporated into the viscosity definition, then the length, time, pressure, viscosity, concentrations of the chemical species, concentration of NPs, and velocity were scaled with $\frac{D_a \phi}{U}$, $\frac{D_a \phi^2}{U^2}$, $D_a \phi \mu_{a_0}$, μ_{a_0}, C_0, C_{n0}, and U, respectively. D_a is the diffusion coefficient of component A, and ϕ is the medium porosity. The ratios of the diffusion coefficients of the corresponding components with respect to that of component A are denoted by δ_j and δ_n. $\mathrm{Da} = k_R D_a \phi^2 C_0 C_{n0}/U^2$ is the Damköhler number, defined as the ratio of the diffusion to reaction timescales; $\mathrm{Da}_{dep} = k_{dep} D_a \phi^2/U^2$ is defined as the ratio of the diffusion to deposition timescales, hence representing the deposition rate of NPs. In the previous expressions, k_R is the reaction rate constant, while k_{dep} is the deposition rate coefficient, following the widely applied colloid filtration theory (CFT) [19]. According to the CFT, k_{dep} is constant and does not consider the detachment of the particles from the solid matrix. With the introduced scaling, the dimensions of the computational domain are $(-\frac{\mathrm{Pe}}{2}, \frac{\mathrm{Pe}}{2})$ in the

x direction and $(0, \frac{\mathrm{Pe}}{A_s})$ in the y direction, where $\mathrm{Pe} = UL/D_a\phi$ is the Péclet number, and $A_s = L/W$ is the aspect ratio.

Using a proper linearly moving reference frame and setting Pe large enough, the concentrations of A, B, and NPs obey the zero-flux condition at the x boundaries, while the velocity and C_c are zero. Moreover, periodic boundary conditions are adopted in the y direction. In addition, the Heaviside step function (H) is used in the form of $C_a = H(-x)$, $C_b = H(x)$, and $C_n = C_{n_0}H(-x)$ for the initial concentrations of components A, B, and NPs, respectively. Both the concentration of the chemical product C and the velocity in the moving reference frame are initially zero. The model is completed by adopting the following widely used exponential viscosity-concentration relationship [9,15,20]:

$$\mu = \exp(R_bC_b + R_cC_c + R_nC_n), \tag{5}$$

where R_b, R_c, and R_n are the viscosity ratios with respect to the component A, defined as

$$R_b = \ln\left(\frac{\mu_{b_0}}{\mu_{a_0}}\right), \quad R_c = \ln\left(\frac{\mu_{c_0}}{\mu_{a_0}}\right), \quad R_n = \ln\left(\frac{\mu_{n_0}}{\mu_{a_0}}\right). \tag{6}$$

Although this exponential viscosity model is a theoretical assumption, Tan and Homsy [21] could successfully apply it to predict the stability condition, as well as the order of magnitude of both the wavelength of the instabilities and the finger width of the experimental work by Slobod and Thomas [22]. After eliminating the pressure by taking the curl of Eq. (2), six sets of dimensionless governing equations are solved numerically with a pseudospectral method [23].

IV. RESULTS AND DISCUSSION

The research goal is to elucidate the role of NP deposition on the flow dynamics, the VF instability, and the total chemical product. It should be first stressed that hereafter the term "intrinsically unstable" and "intrinsically stable" refer to the stability condition of the NP-laden systems in the absence of deposition before the reaction.

Under constant and identical diffusivities of all chemical components, which is the focus of the present study, the system is intrinsically unstable if $R_n < R_b$, whereas it is intrinsically stable when $R_n \geqslant R_b$ [24]. After the reaction, the new product with the viscosity ratio R_c is produced in the presence of nanocatalysts. For the case of $\mathrm{Da}_{dep} = 0$, it has been reported that the intrinsically unstable system remains unstable after the reaction regardless of the value of R_c. However, depending on the value of R_c the intrinsically stable system may remain stable or become unstable after the reaction [10]. Specifically, the reactive NP-laden system is stable in the absence of deposition when both $2R_b - R_c - R_n \leqslant 0$ and $R_c - R_n < 0$, otherwise it is unstable. Moreover, the intrinsically unstable system is less unstable after the reaction, while the intrinsically stable one is still stable when $R_c = R_b$. Therefore, at $R_c = R_b$, the total amount of chemical product is minimal as well in both intrinsically unstable and stable systems. As $|R_c - R_b|$ increases, both systems are prone to more unstable situation with more chemical product. More precisely, it was found that as R_c increases, the system first becomes less unstable and the total chemical product decreases till $R_c = R_b$. Further increasing R_c makes the flow subject to more unstable state and results in more chemical product.

In the present study, we will show that NP deposition changes the dynamics, since the reaction rate $r_R = \mathrm{Da}C_aC_bC_n$ is a function of NP concentration. Such linear dependency of the reaction rate on the nanocatalyst concentration has been reported in previous experimental studies [25–28] and, hence, is used in our study. In the following, the effect of NP deposition will be investigated for both the intrinsically unstable and intrinsically stable systems. The analysis will be conducted qualitatively with the contours of C_c and C_a and quantitatively by calculating the normalized total amount of the chemical product, $(C_c)_t$, at each time (t), which is defined as

$$(C_c)_t(t) = \frac{A_s}{\mathrm{Pe}^2}\int_{-\frac{\mathrm{Pe}}{2}}^{\frac{\mathrm{Pe}}{2}}\int_0^{\frac{\mathrm{Pe}}{A_s}} C_c(x, y, t)\, dy\, dx. \tag{7}$$

In the simulations, $\mathrm{Da} = 1$, $\mathrm{Pe} = 4096$, and $A_s = 8$ are used and fixed unless stated otherwise, while the diffusivities are set to unity, $\delta_j = \delta_n = 1$, to avoid double diffusive effects. In addition, the viscosity ratios of $(R_b = 3,\ R_n = 2)$ and $(R_b = -0.5,\ R_n = 2)$ are used to represent the intrinsically unstable and intrinsically stable systems, respectively. Last but not least, the numerical convergence was checked, and the grid number of 512×256 was found to be satisfactory. In addition, to validate our code the results were benchmarked with the available numerical results for NP-free nonreactive systems, by setting our simulation with $R_c = R_n = \mathrm{Da} = \mathrm{Da}_{dep} = 0$. Moreover, the finger configurations of NP-free reactive systems reported by Ref. [17] were compared with the results of the developed code by setting $R_n = \mathrm{Da}_{dep} = 0$ and $C_n = 1$. In both cases our simulation results show good agreement.

A. Intrinsically unstable systems

In the presence of NP deposition, one may think that since C_n decreases over time upon deposition, the reaction rate $r_R = \mathrm{Da}C_aC_bC_n$ and hence the rate of total chemical product, $(\dot{C_c})_t \equiv \frac{d(C_c)_t}{dt}$, would decrease. However, our simulation results of $(\dot{C_c})_t$ shows that the trend is actually not always monotonically decreasing with time. Instead, as shown in Fig. 2 for a representative intrinsically unstable system $(R_c = 1, \mathrm{Da}_{dep} = 0.008)$, four different regimes are generally observed in the passage of time.

The first phase is a "diffusive" regime where the flow is stable, while the production rate is decreasing. The second one is "mixing-dominant fingering" regime where the production rate is generally increasing due to the significant mixing of flow resulting from the VF instabilities. The subsequent third is the "transition" regime where the production rate is again generally decreasing. The final, fourth regime is a "zero-production" regime where no further production is observed, while the product diffuses and decays. This generic trend of the four regimes is observed at all the adopted R_c in various intrinsically unstable systems with $R_n > 0$. Since the rate of chemical product may not be always monotonic in the mixing-dominant fingering and the transition regimes, we used the term "general" to describe the trends. The transitional time

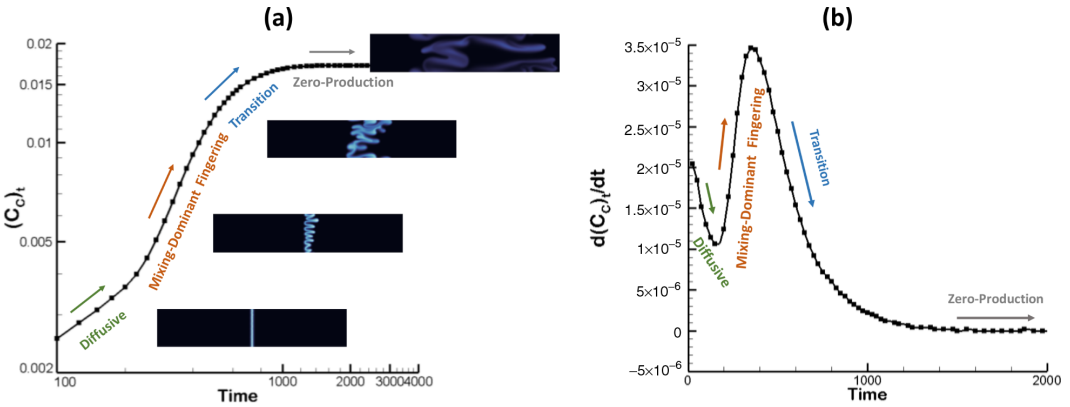

FIG. 2. The general trends of (a) the variation of total amount of chemical product in log-log scale and (b) the rate change of total amount of chemical product with time, in an intrinsically unstable system with $R_c = 1$, $\mathrm{Da}_{dep} = 0.008$. The snapshots are the contours of C_c at $t = 100, 300, 600$, and 1500, corresponding to each of the four generic regimes observed: diffusive, mixing-dominate, transition, and zero-production, respectively.

between those regimes is found to be a function of all the variables and, most importantly, dependent on the deposition rate. We hence analyze the effect of Da_{dep} on the variation of $(C_c)_t$.

Figure 3 shows the influence of Da_{dep} on the total amount of chemical product, $(C_c)_t$, in an intrinsically unstable system with $R_c = 1$. Initially, the nanocatalytic reaction takes place as the fluids approach, and the product initially transports in a diffusive regime. In this regime, $(C_c)_t$ increases with $t^{1/2}$ [29] in the absence of deposition, while its rate decreases as $t^{-1/2}$. In the presence of NP deposition, the reaction rate decreases continuously, and accordingly the variation of $(C_c)_t$ with time deviates slightly from $t^{1/2}$. After the diffusive regime, the chemical product always increases with time when $\mathrm{Da}_{dep} = 0$. However, in the presence of deposition, the total amount of chemical product first increases and then after a transition period becomes constant, following the regimes discussed

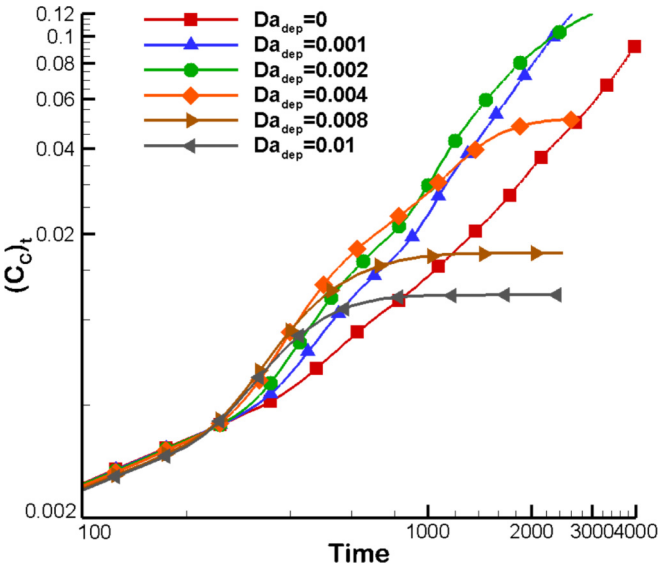

FIG. 3. Variation of the total amount of chemical product, $(C_c)_t(t)$, over time at different deposition rates, Da_{dep}, in the intrinsically unstable system with $R_c = 1$, plotted in a log-log scale.

in Fig. 2. As illustrated in Fig. 3, in the mixing-dominant fingering regime, the chemical product increases with Da_{dep}. However, both the final amount of chemical product and its value in the transition regime are lower at higher deposition rates. The period in which the system is actually in the mixing-dominant fingering regime is shortened at higher Da_{dep}. Hence, at very large deposition rates the system may bypass the mixing-dominant fingering regime and transition to the zero-production regime. Interestingly, due to the different transition times between the various regimes in Fig. 3, it seems that in a period of time, $(C_c)_t$ first increases and then decreases with deposition. It is worth stressing that similar trends were observed in other intrinsically unstable systems as well.

To explain the response of the system to NP deposition, we first analyze the one-dimensional viscosity variation along the channel. With the boundary and initial conditions specified, one can show the following relations between the one-dimensional concentration of different components, NPs, A, B, and C: $\bar{C}_n = \frac{C_{n_0}}{2}\mathrm{erfc}(\frac{x}{2\sqrt{t}})\exp(-\mathrm{Da}_{dep}t)$, $\bar{C}_a + \bar{C}_b + 2\bar{C}_c = 1$, and $\bar{C}_b - \bar{C}_a = \mathrm{erf}(\frac{x}{2\sqrt{t}})$. Here $\mathrm{erf}(\eta)$ and $\mathrm{erfc}(\eta)$ are the error function and complementary error function, respectively. After some manipulation, and finally substituting $C_{n_0}R_n$ by R_n, the following expression of the first derivative of the one-dimensional viscosity, $\bar{\mu}$, is obtained:

$$\frac{2}{\bar{\mu}}\frac{\partial\bar{\mu}}{\partial x} = (R_c - R_n e^{-\mathrm{Da}_{dep}t})\left(-\frac{\partial\bar{C}_a}{\partial x}\right) + (2R_b - R_c - R_n e^{-\mathrm{Da}_{dep}t})\frac{\partial\bar{C}_b}{\partial x}. \quad (8)$$

Since $(-\frac{\partial\bar{C}_a}{\partial x})$ and $\frac{\partial\bar{C}_b}{\partial x}$ are both positive, one can consider two zones in the system, namely, the trailing (T) and the leading (L) ones, each with an effective viscosity ratio of $R_T = R_c - R_n e^{-\mathrm{Da}_{dep}t}$ and $R_L = 2R_b - R_c - R_n e^{-\mathrm{Da}_{dep}t}$, respectively. This indicates that in the presence of deposition, the effective nanofluid viscosity ratio is $R_n e^{-\mathrm{Da}_{dep}t}$ instead, and the effect of R_n decreases with time. In the intrinsically unstable system ($R_n < R_b$) with $\mathrm{Da}_{dep} = 0$, either $2R_b - R_c - R_n > 0$ or $R_c - R_n > 0$ or both. This means that in such

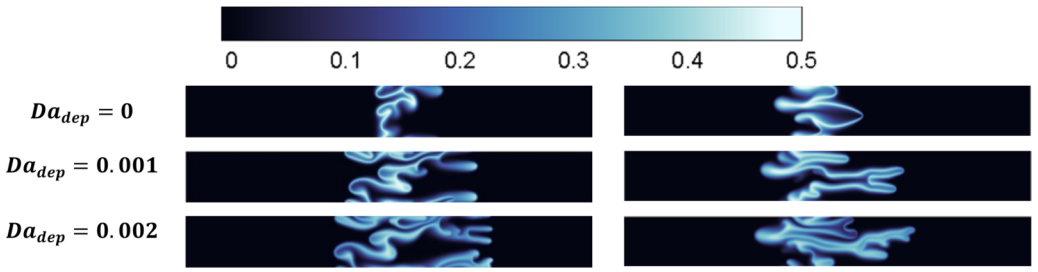

FIG. 4. Contours of C_c at different deposition rates, Da_{dep} in two intrinsically unstable systems, with $R_c = 1$ (left) and $R_c = 7$ (right); $t = 1500$.

systems, at least one of the zones will be unstable after the reaction. Accounting for the NP deposition, the effective R_n decreases with time, and thus the effective viscosity ratios of each zone increases. The increase in R_T and/or R_L implies a more unstable situation and more chemical product regardless of the value of R_c. This explains why the chemical product increases with Da_{dep} in the mixing-dominant fingering regime. In other words, the increase in the production rate, as a result of an increase in mixing, overcomes the continuous decrease of the reaction rate. The more complex finger configuration with increasing deposition rate is well illustrated in Fig. 4 for the intrinsically unstable system, for two values of $R_c = 1$ and $R_c = 7$.

In an opposite trend compared to the mixing-dominant fingering regime, the rate of chemical production, $(\dot{C}_c)_t$, in the transition regime decreases with deposition, Da_{dep}. At sufficiently large times and/or for larger values of the deposition rates, where the system is in the transition regime, the concentration of NPs is low, and as a result the decrease in the reaction rate overcomes the effect of mixing resulting from the VF instabilities. In this regime, the concept of trailing and leading zones does not hold, and the effect of the chemical products on the viscosity is reduced compared to the case when $\mathrm{Da}_{dep} = 0$. To show this decreasing effect, using $\bar{C}_a + \bar{C}_c = \frac{1}{2}\mathrm{erfc}(\frac{x}{2\sqrt{t}})$ and $\bar{C}_b + \bar{C}_c = \frac{1}{2}\mathrm{erfc}(\frac{-x}{2\sqrt{t}})$, Eq. (8) is written as below after eliminating $\bar{C}_a$ and $\bar{C}_b$:

$$\frac{1}{\bar{\mu}}\frac{\partial \bar{\mu}}{\partial x} = (R_b - R_n e^{-\mathrm{Da}_{dep}t})\frac{1}{2\sqrt{\pi t}}e^{-\frac{x^2}{4t}} + (R_c - R_b)\frac{\partial \bar{C}_c}{\partial x}. \tag{9}$$

The first term in the RHS appears in NP-laden nonreactive systems, while the second one arises as a result of the reaction. Since Eq. (9) involves the concentration of the product, it is valuable to derive the transport equation of the component C. Eliminating $\bar{C}_a$ and $\bar{C}_b$ from Eq. (3) and substituting $\bar{C}_n = \frac{C_{n_0}}{2}\mathrm{erfc}(\frac{x}{2\sqrt{t}})\exp(-\mathrm{Da}_{dep}t)$, one will obtain the following equation after some manipulation, by substituting $\mathrm{erfc}(\frac{x}{2\sqrt{t}})\mathrm{erfc}(\frac{-x}{2\sqrt{t}}) = 1 - \mathrm{erf}^2(\frac{x}{2\sqrt{t}}) \sim e^{-\frac{x^2}{4t}}$ and simply assuming $C_{n_0} = 1$:

$$\frac{\partial \bar{C}_c}{\partial t} = \frac{\partial^2 \bar{C}_c}{\partial x^2} + \frac{\mathrm{Da}}{2}\left(\bar{C}_c{}^2 - \frac{\bar{C}_c}{2} + \frac{e^{-\frac{x^2}{4t}}}{4}\right)\mathrm{erfc}\left(\frac{x}{2\sqrt{t}}\right)e^{-\mathrm{Da}_{dep}t}. \tag{10}$$

Equation (10) is a modified Fisher's equation and does not have an analytic solution. The first term in the RHS of Eq. (10) is diffusive, while the second is a source or sinkliked term. In the presence of deposition, as time passes, the effect of the source term decreases exponentially, with a decay rate of Da_{dep}. Meanwhile, the already produced product is diffusing and fading away via the $\frac{\partial^2 \bar{C}_c}{\partial x^2}$ term. Large times and/or higher deposition rates intensify this exponential decaying process, whereas increasing Da works in an opposite way. The fading effect due to the diffusive term and the decaying of the source term indicate a reduction in the absolute value of $\frac{\partial \bar{C}_c}{\partial x}$. Therefore, the effect of $(R_c - R_b)\frac{\partial \bar{C}_c}{\partial x}$ on the viscosity is gradually diminishing, indicating a reduced effect of the chemical product on the dynamics and a gradual collapse in the zones. Since the effect of R_n is decreasing simultaneously as well, one may conclude that in the transition regime the viscosity distribution is getting more affected by $R_b\frac{1}{2\sqrt{\pi t}}e^{-\frac{x^2}{4t}}$, and accordingly the dynamics of the solutions is gradually dominating the flow.

Finally, it is clear that at large enough time, where the system is in the final regime, the NPs have been totally deposited and hence catalytically removed from the system. As a consequence, the reaction comes to an end, and the product diffuses and fades away completely over time. Note that the system will ultimately reduce to a binary flow where the dynamics is governed only by the transport of the reactants. Therefore, assuming $R_n \geqslant 0$, which is the focus of the present study, the intrinsically unstable system ($R_n < R_b$) is ultimately unstable as well. The contours of C_c and C_a in Fig. 5 shows that the intensity of the product concentration (C_c) is reduced with time, as a result of the reduction in the reaction rate, and fading away. Figure 5 further reveals that the fingering patterns for both components, C_a and C_c, become similar at large time, indicating the domination of the reactants on the flow dynamics.

There is one more factor in Eq. (10) that is worth mentioning. The existence of the complementary error function in the source term indicates that $\bar{C}_c(x,t)$ is not symmetric in the nanocatalytic reactions, so the product is larger at $x < 0$ where NPs are abundant. This is in contrast with the NP-free reactive systems where $\bar{C}_c(x,t)$ is symmetric.

B. Intrinsically stable systems

In the absence of deposition ($\mathrm{Da}_{dep} = 0$), the intrinsically stable system ($R_b \leqslant R_n$) may become unstable or remain stable after the reaction. For brevity, these systems will be

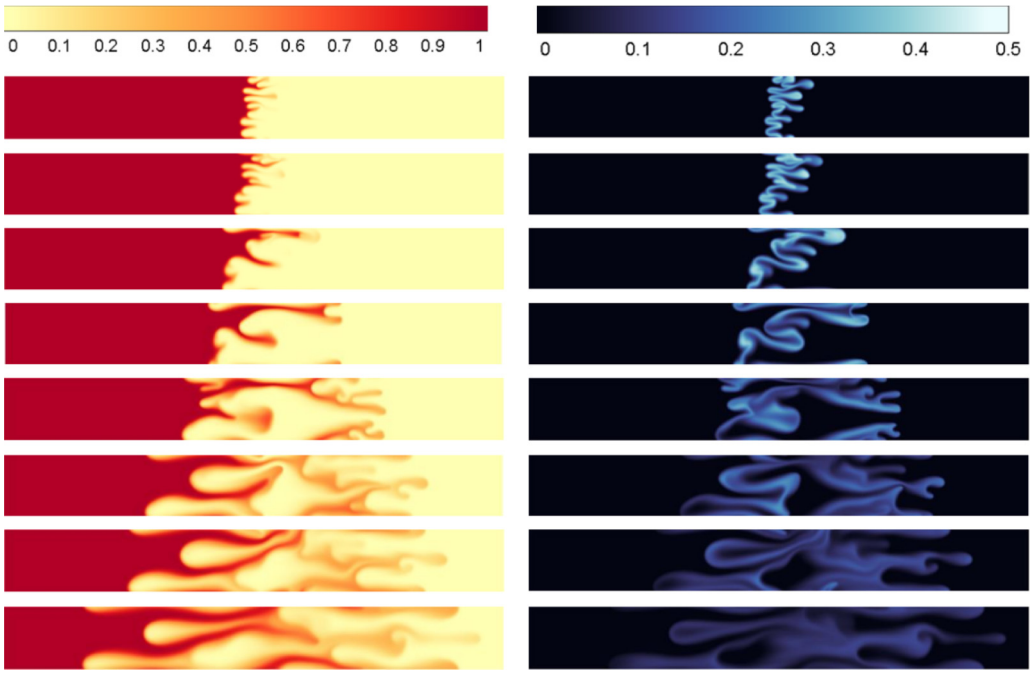

FIG. 5. Contours of C_a (left) and C_c (right) in the intrinsically unstable system with $R_c = 1$ and $\mathrm{Da}_{dep} = 0.004$. The corresponding time of the snapshots: $t = 500$, 600, 800, 1000, 1400, 1800, 2000, and 2500 from the top to bottom, respectively.

called "intrinsically stable-unstable" and "intrinsically stable-stable," respectively. On one hand, in the intrinsically stable-stable systems, both trailing and leading zones after the reaction are stable, i.e., $2R_b - R_c - R_n \leqslant 0$ and $R_c - R_n < 0$ [10]. On the other hand, in the intrinsically stable-unstable systems one of the zones becomes unstable after the reaction: $(2R_b - R_c - R_n)(R_c - R_n) < 0$ [10]. The analysis of $(C_c)_t$(t), which is not shown here for brevity, indicates that the response of the intrinsically stable-unstable systems to the deposition is similar to that discussed concerning the intrinsically unstable systems in Fig. 2. More precisely, there is a period of time where $(C_c)_t$ first increases with increase of the deposition rate, following a later decrease. In addition, the values of $(C_c)_t$ in the mixing-dominant fingering regime increase with Da_{dep}, whereas the opposite trend is observed in the transition and zero-production regimes.

The intrinsically stable-stable systems, however, respond to the deposition rate in two different ways. In some cases, illustrated in Fig. 6, the response is similar to that observed in the intrinsically unstable systems. However, there are other cases, where $(C_c)_t$ always decreases with the deposition rate. In other words, in the latter case the mixing-dominant fingering regime does not occur, and, thus, the rate of change of $(C_c)_t$ is negative for all deposition rates till it reaches zero at later time. Although the system in Fig. 6(a) is intrinsically stable-stable, an increase in the production rate after the diffusive regime at moderate deposition rates indicates that this system experiences the mixing-dominant fingering regime. In other words, one can conclude that first, the intrinsically stable-stable systems may become unstable as a result of deposition; second, the resulting mixing may overcome the effect of the reduction in the reaction rate, leading to an increase in the production rate. Shown in Fig. 6(a), after a critical Da_{dep} the system will never experience the mixing-dominant fingering regime, and the production rate decreases with deposition. Note that not experiencing the mixing-dominant fingering regime does not necessarily imply a stable system. It, however, indicates that the reduction in the reaction rate as a result of the deposition is always dominant on the rate of chemical product, regardless of whether the system is stable or unstable.

Figure 7 shows contours of C_c at different deposition rates in the intrinsically stable-stable systems illustrated in Fig. 6. The system in Fig. 7(a) is unstable at $\mathrm{Da}_{dep} = 0.001$. This system is unstable at $\mathrm{Da}_{dep} = 0.004$ as well; however, as shown in Fig. 6(a), the instabilities cannot overcome the reduction in the reaction rate to increase $(C_c)_t$. On the other hand, in those intrinsically stable-stable systems where the deposition decreases only the production rate, the system is always stable, as illustrated by the contours of C_c in Fig. 7(b).

Based on the results and discussion in Sec. IV A, the increase in the production rate occurs only when the system is in the mixing-dominant fingering regime, where the concept of leading and trailing zones and their effective viscosity is helpful. In the intrinsically stable-unstable systems, either $2R_b - R_c - R_n > 0$ or $R_c - R_n > 0$. In the presence of deposition, the effective viscosity ratio, $R_{n,\mathrm{eff}} = R_n e^{-\mathrm{Da}_{dep} t}$. Therefore, moderate deposition rates gradually decrease $R_{n,\mathrm{eff}}$ and increase viscosity ratio of each zone, hence intensify the mixing, and increase $(\dot{C}_c)_t$ at moderate time, similar to the mechanisms discussed for the intrinsically unstable system. Larger deposition rates and/or larger time lead to the dominance of the reduction in the reaction rate over mixing and, hence, the reduction in the production rate.

In the intrinsically stable-stable systems, $2R_b - R_c - R_n \leqslant 0$ and $R_c - R_n < 0$. Accounting for the deposition makes either of the viscosity ratios of the zones positive with time, if

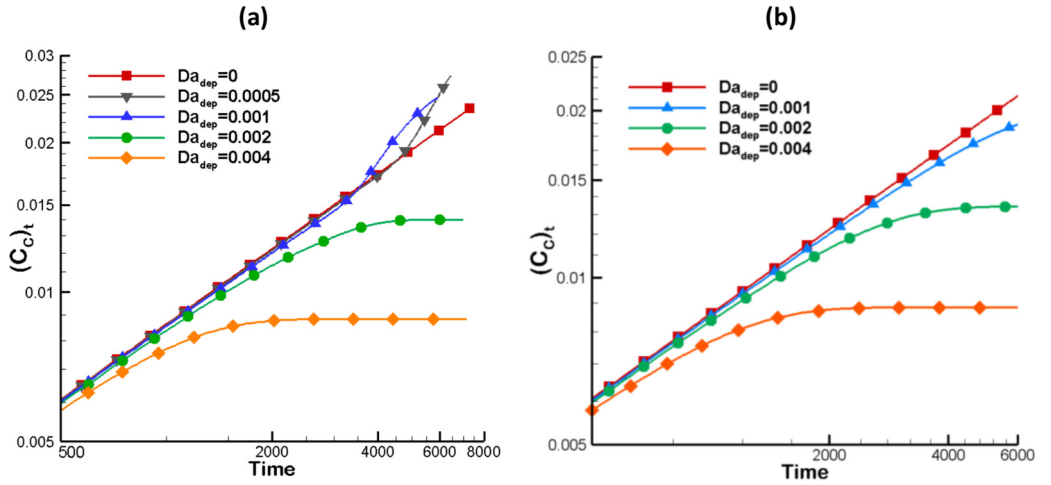

FIG. 6. Variation of the total amount of chemical product, $(C_c)_t$, with deposition rate, Da_{dep}, in two intrinsically stable systems: (a) $R_c = -3$, and (b) $R_c = -0.5$, plotted in a log-log scale.

$0 < 2R_b - R_c \leqslant R_n$ or $0 < R_c \leqslant R_n$. This explains why the intrinsically stable-stable system with $R_c = -3$ became unstable as a consequence of deposition, but not for the case of $R_c = -0.5$.

The same mechanisms and discussion in Sec. IV A about the transition regime and the final zero-production regime are still valid and applicable for intrinsically stable-unstable and intrinsically stable-stable systems as well. Accordingly, both the intrinsically stable-unstable and the intrinsically stable-stable systems are ultimately stable since $R_b < R_n$.

C. Systems where $R_n = 0$

All the above-mentioned discussion in the previous sections regarding an increase in the production rate as a result of deposition is not valid when $R_n = 0$. Conversely, our simulation data show that the production rate decreases and subsequently becomes zero in both intrinsically unstable and intrinsically stable systems with $R_n = 0$. This is because the deposition does not have any effect on the effective nanofluid viscosity ratio when $R_n = 0$, according to Eq. (8). As a result, these systems will not experience the mixing-dominant fingering regime. Instead, the constant reduction in the reaction rate as a result of deposition reduces the production rate till it reaches zero.

V. CONCLUSION

Flow dynamics and total amount of chemical products, $(C_c)_t$, are investigated when two fluids meet and react in a porous medium in the presence of nanocatalysts (NPs). The invading fluid A and displaced fluid B undergo a chemical reaction of $\mathrm{A} + \mathrm{B} + \mathrm{n} \rightarrow \mathrm{C} + \mathrm{n}$, while the NPs, originally dispersed in the fluid A, are deposited continuously in the medium. In the absence of deposition ($\mathrm{Da}_{dep} = 0$), the systems are first categorized as "intrinsically unstable" (unstable before and after the reaction), "intrinsically stable-unstable" (stable before the reaction while unstable after the reaction), and "intrinsically stable-stable" (stable before and after the reaction). Their responses to the NPs deposition is subsequently analyzed.

Due to the continuous decrease in the NP concentration upon deposition, the final $(C_c)_t$ decreases with increasing Da_{dep}. However, one factor that may overcome this decreasing effect and make the chemical product increase in an intermediate time was identified. This positive factor is associated with the effective mixing of the components as a result of the onset or the enhancement of the VF instabilities due to the viscosity modification after the deposition.

The study illustrates that the system generally undergoes four generic regimes over time in response to the NP

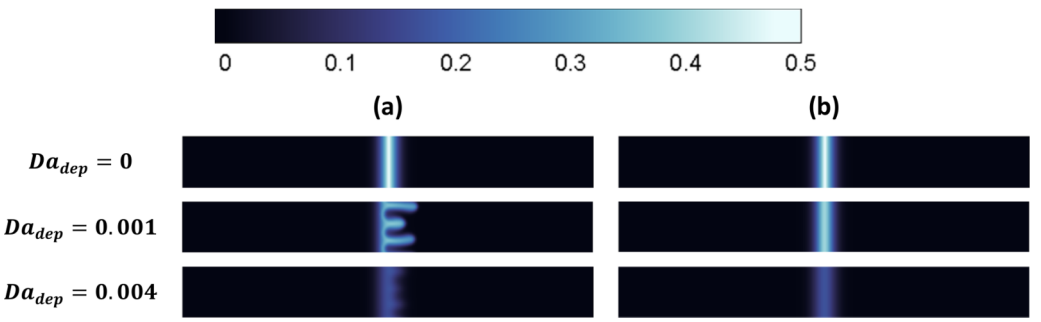

FIG. 7. Contours of C_c at different deposition rates, Da_{dep}, in the intrinsically stable-stable system for (a) $R_c = -3$ and (b) $R_c = -0.5$; Here $t = 4000$.

deposition, in the sequence of diffusive, mixing-dominant fingering, transition, and zero-production. In the initial diffusive regime, the chemical product diffuses along the channel with other components, while the rate of production decreases with time. In contrast to systems undergoing $A + B \rightarrow C$ reaction, in this diffusive regime the chemical product is abundant in the upstream region of the flow, $x < 0$. In the subsequent mixing-dominant fingering regime, the VF instabilities are developed or intensified due to the deposition and lead to an increase in the production rate, despite the reductions of both the NP concentration and the reaction rate. To understand and explain this trend, the concept of trailing and leading zones was employed. The NP deposition increases the viscosity ratio of each zone and makes the system more prone to instabilities. This regime is observed at moderate deposition rates and in a limited period. An increasing deposition rate reduces the period that this regime is effective, while the Damköhler number (Da) acts in an opposite way. Therefore, it is expected that at sufficiently large Da_{dep} or small enough Da, the mixing-dominant fingering regime may be simply eliminated. Interestingly, this regime is observed in all the classified systems except two groups: first, those in which the nanocatalysts do not change the viscosity of the base fluid ($R_n = 0$) and, second, a subgroup of intrinsically stable-stable systems. In the third transition regime, the concentration of nanocatalysts is low, the reduction in the reaction rate overcomes the flow mixing condition, and the production rate decreases. In this regime, the flow may be stable or unstable, the product gradually loses its effect on the viscosity, the concept of two zones gradually collapses, and the effect of R_b (the viscosity ratio of the solutions) gradually dominates the flow. In the fourth and last identified zero-production regime, the concentration of the NPs and the reaction rate are zero. Then the already produced product diffuses along the channel and gradually fades away. Ultimately, the dynamics are governed only by the reacting fluids.

ACKNOWLEDGMENTS

Support from the University of Calgary's Eyes High Scholarship program is acknowledged. The authors also acknowledge the Natural Sciences and Engineering Research Council of Canada (NSERC), Alberta Innovates, and computing resources of the West-Grid clusters. P.A.T. holds a Canada Research Chair in Fluids and Interfaces and acknowledges funding from NSERC.

[1] V. Shashikala, V. S. Kumar, A. H. Padmasri, B. D. Rajua, S. V. Mohan, P. Nageswara Sarma, and K. S. Rama Rao, Advantages of nano-silver-carbon covered alumina catalyst prepared by electro-chemical method for drinking water purification, J. Mol. Catal. A: Chem. **268**, 95 (2007).

[2] H. S. Oh, J. G. Oh, Y. G. Hong, and H. Kim, Investigation of carbon-supported Pt nanocatalyst preparation by the polyol process for fuel cell applications, Electrochim. Acta **52**, 7278 (2007).

[3] R. S. Singh, V. K. Rangari, S. Sanagapalli, V. Jayaraman, S. Mahendra, and V. P. Singh, Nano-structured CdTe, CdS and TiO_2 for thin film solar cell applications, Sol. Energy Mater. Sol. Cells **82**, 315 (2004).

[4] L. Wen, Y. Wang, D. Lu, S. Hu, and H. Han, Preparation of KF/CaO nanocatalyst and its application in biodiesel production from Chinese tallow seed oil, Fuel **89**, 2267 (2010).

[5] R. Hashemi, N. N. Nassar, and P. Pereira Almao, Enhanced heavy oil recovery by *in situ* prepared ultradispersed multimetallic nanoparticles: A study of hot fluid flooding for Athabasca bitumen recovery, Energy Fuels **27**, 2194 (2013).

[6] J. B. Omajali, A. Hart, M. Walker, J. Wood, and L. E. Macaskie, *In-situ* catalytic upgrading of heavy oil using dispersed bio-nanoparticles supported on gram-positive and gram-negative bacteria, Appl. Catal., B **203**, 807 (2017).

[7] M. C. Chang, H. Y. Shu, W. P. Hsieh, and M. C. Wang, Using nanoscale zero-valent iron for the remediation of polycyclic aromatic hydrocarbons contaminated soil, J. Air Waste Manage. Assoc. **55**, 1200 (2005).

[8] N. Sabet, S. M. Jafari Raad, H. Hassanzadeh, and J. Abedi, Dynamics of Miscible Nanocatalytic Reactive Flows in Porous Media, Phys. Rev. Appl. **10**, 054033 (2018).

[9] K. Ghesmat, H. Hassanzadeh, J. Abedi, and Z. Chen, Frontal stability of reactive nanoparticle transport during *in situ* catalytic upgrading of heavy oil, Fuel **107**, 525 (2013).

[10] B. Dastvareh and J. Azaiez, Instabilities of nonisothermal nanocatalytic reactive flows in porous media, Phys. Rev. Fluids **4**, 034003 (2019).

[11] A. De Wit and G. M. Homsy, Viscous fingering in reaction-diffusion systems, J. Chem. Phys. **110**, 8663 (1999).

[12] A. De Wit and G. M. Homsy, Nonlinear interactions of chemical reactions and viscous fingering in porous media, Phys. Fluids **11**, 949 (1999).

[13] T. Podgorski, M. C. Sostarecz, S. Zorman, and A. Belmonte, Fingering instabilities of a reactive micellar interface, Phys. Rev. E **76**, 016202 (2007).

[14] Y. Nagatsu, K. Matsuda, Y. Kato, and Y. Tada, Experimental study on miscible viscous fingering involving viscosity changes induced by variations in chemical species concentrations due to chemical reactions, J. Fluid Mech. **571**, 475 (2007).

[15] S. H. Hejazi, P. M. J. Trevelyan, J. Azaiez, and A. De Wit, Viscous fingering of a miscible reactive $A + B \rightarrow C$ interface: A linear stability analysis, J. Fluid Mech. **652**, 501 (2010).

[16] V. Sharma, S. Pramanik, C. Y. Chen, and M. Mishra, A numerical study on reaction-induced radial fingering instability, J. Fluid Mech. **862**, 624 (2019).

[17] S. H. Hejazi and J. Azaiez, Non-linear interactions of dynamic reactive interfaces in porous media, Chem. Eng. Sci. **65**, 938 (2010).

[18] Y. Nagatsu and A. De Wit, Viscous fingering of a miscible reactive $A + B \rightarrow C$ interface for an infinitely fast chemical reaction: Nonlinear simulations, Phys. Fluids **23**, 043103 (2011).

[19] K. M. Yao, M. T. Habibian, and C. R. O'Melia, Water and waste water filtration: Concepts and applications, Environ. Sci. Technol. **5**, 1105 (1971).

[20] C. T. Tan and G. M. Homsy, Simulation of nonlinear viscous fingering in miscible displacement, Phys. Fluids **31**, 1330 (1988).

[21] C. T. Tan and G. M. Homsy, Stability of miscible displacements in porous media: Rectilinear flow, Phys. Fluids **29**, 3549 (1986).

[22] R. L. Slobod and R. A. Thomas, Effect of transverse diffusion on fingering in miscible-phase displacement, Soc. Pet. Eng. J. **3**, 9 (2007).

[23] M. N. Islam and J. Azaiez, Fully implicit finite difference pseudo-spectral method for simulating high mobility-ratio miscible displacements, Int. J. Numer. Methods Fluids **47**, 161 (2005).

[24] B. Dastvareh and J. Azaiez, Instabilities of nanofluid flow displacements in porous media, Phys. Fluids **29**, 044101 (2017).

[25] P. L. Freund and M. Spiro, Colloidal catalysis: The effect of sol size and concentration, J. Phys. Chem. **89**, 1074 (1985).

[26] H. N. McMurray, Particle size effects in electrocatalysis by uniform colloids of ruthenium dioxide hydrate, J. Phys. Chem. **98**, 9861 (1994).

[27] Y. Li, X. M. Hong, D. M. Collard, and M. A. El-Sayed, Suzuki cross-coupling reactions catalyzed by palladium nanoparticles in aqueous solution, Org. Lett. **2**, 2385 (2000).

[28] S. Carregal-Romero, J. Prez-Juste, P. Hervs, L. M. Liz-Marzn, and P. Mulvaney, Colloidal gold-catalyzed reduction of ferrocyanate (III) by borohydride ions: A model system for redox catalysis, Langmuir **26**, 1271 (2009).

[29] C. M. Gramling, C. F. Harvey, and L. C. Meigs, Reactive transport in porous media: A comparison of model prediction with laboratory visualization, Environ. Sci. Technol. **36**, 2508 (2002).